BBAA VI International Colloquium on:
Bluff Bodies Aerodynamics & Applications
Milano, Italy, July, 20-24 2008

FULL-SCALE AERODYNAMIC MEASUREMENTS UNDERNEATH A HIGH SPEED TRAIN

Andrew Quinn[*] and Mick Hayward[*†]

[*]Department of Civil Engineering
University of Birmingham, Edgbaston, Birmingham, UK
e-mail: A.D.Quinn@bham.ac.uk,

[†] CTRL, Network Rail
40 Melton Street, London, UK
e-mail: Mick.Hayward@networkrail.co.uk

Keywords: Railway, HSR, Transport, Ballast flight, Pressure, Air speed.

1 INTRODUCTION

Damage to the rail running surface, known in the industry as the railhead, has long been known to occur and is a major maintenance cost on any rail network [1]. Various forms of railhead damage have been identified including rail breakage, traffic initiated wear and fatigue initiated surface cracks. Many of these forms are now collectively referred to as Rolling Contact Fatigue (RCF) and mitigation measures include railhead surface grinding and lubrication [2, 3]. With the development of high-speed rail (HSR) systems another form of railhead damage, known as "ballast pitting", has become apparent and is illustrated in Fig. (1).

It is hypothesised that this form of damage is due to small particles of ballast being crushed between the railhead and the wheels of rail vehicles. This form of damage becomes more apparent on HSR networks because of the speed and energy of the vehicle, which is thought to generate an explosive crushing of the ballast particle, which damages the railhead. The effect is also more significant on HSR networks because the forces involved are large enough to cause permanent deformation of the rail, which in turn leads to "voiding", the formation of hollow areas in the ballast between the sleepers, which affects the track stability. Experience on the Channel Tunnel Rail Link (CTRL) suggests that such voids reoccur if the underlying rail deformation is not corrected and that a series of such voids can form "downstream" of an uncorrected deformation. It is assumed that both aerodynamic and mechanical factors play a role in this issue but the detailed mechanisms for void generation, and the initial ballast pitting, are not clearly understood.

As an initial investigation into these issues this paper describes a series of observations and measurements made on the Channel Tunnel Rail Link (CTRL) HSR track in the UK as part of an MSc dissertation project. The CTRL is the first purpose built HSR track in the UK and is capable of vehicle speeds up to around 85 ms^{-1} (300 km/h). These observations sought to establish qualitatively and quantitatively the properties of the flow underneath HSR vehi-

cles in order to establish whether they are potentially capable of depositing ballast particles on the railhead thereby initiating the ballast pitting and voiding process.

Previous studies [4, 5, 6] have looked at the aerodynamic features around the sides and roof of high-speed vehicles at both model and full-scale but few measurements of the conditions occurring underneath vehicles, particularly rail vehicles, seem to have been made. The most significant studies have been carried out by [7, 8, 9] in which the under-body air velocities have been measured on different vehicles at both full-scale and model scale. Although the detailed results of these studies cannot be directly compared, for various reasons, there is a broad consensus that under-body flows are sensitive to both the vehicle geometry and under-body roughness. Such conditions may be significantly different from those around the vehicle sides and roof because of the presence of the ground as a containing surface on the flow [10].

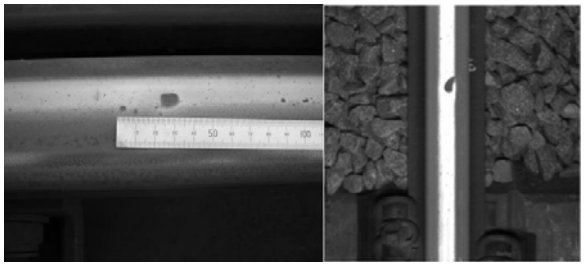

Figure 1 - Ballast pitting damage observed on a HSR railhead (left) and from a train mounted sensor (right)

Section 2 describes the methodology of these studies and section 3 presents a summary of the findings from the second, quantitative, phase of work. These findings are discussed and a direction for future study is proposed in section 4.

2 METHODOLOGY

The site chosen for this study was on the CTRL near Maidstone, Kent (UK grid TQ 8218 5520). This location was selected because it was on a generally straight and level section of track with good access. As such the HSR vehicles, all of which are Eurostar (Class 373 or TGV-TMST) vehicles on this section, are able to pass the location at near maximum speed. The location is also one of the timing locations for the CTRL and therefore the likely schedule of vehicles was well known. The location also houses signalling control gear and therefore power and shelter for the experimental equipment was available. All the observations and measurements were conducted during normal operation of the CTRL and were conducted in full accordance with normal track operational safety procedures. The equipment used was fully certified for use on the rail network prior to the measurements taking place.

Figure 2 - Photograph of initial observations showing lightweight tapes attached to a metal bar on the trackbed shoulder during a Eurostar pass

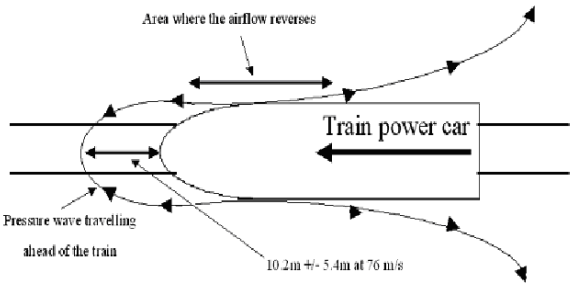

Figure 3 - Illustration of airflow pattern from Phase 1 results. Note that the details represented are limited by the time resolution of the video data to around ± 6m

An initial observation phase was conducted in which lightweight plastic tape strips were fixed to the rail, and on the ballast "shoulder" as shown in Fig. (2), and filmed at 25fps during vehicle passes. These video recordings were analysed frame by

frame to give an air direction and rate of change of direction. This analysis showed that very rapid direction changes were linked to the initial nose region of the flow and to the passing of individual wheel sets. These observations were repeated on sections of canted track (i.e. on curved sections), sections with different surroundings and sections with various widths of ballast "shoulder". All these observations produced results similar to the pattern illustrated in Fig. (3) and therefore it was concluded that the observed effects were entirely due to the passing vehicle and therefore measurements at a single location would be sufficient for the next phase.

In phase 2 the objective was to measure the magnitudes of the pressure and air speed and improve the time resolution of the data. To achieve this 5 pressure transducers [Honeywell 160PC] connected to static pressure probes [11], 4 load cells [Tedea-Huntleigh model 355] and a Cobra Probe [Turbulent Flow Instrumentation Pty Ltd] were mounted on a modified gauge bar which could be bolted across the track as shown in Fig. (4). These instruments gave static pressure, load on a representitive piece of ballast in the trackbed and air speed respectively. The Cobra Probe was moved to 4 positions across the track during the course of the measurements whereas the pressure probes and load cells remained at fixed positions. An additional 2 pressure probes and transducers, mounted at the side of the track equidistant up and down of the instrumented bar, gave an independent measure of vehicle speed.

The data from the pressure transducers and load cells were collected via an analogue-to-digital converter card [Measurement Computing PC-DAS16/16] at 1000 samples per second using purpose written software on a laptop computer. The data from the Cobra Probe were collected at 1250 samples per second using proprietary software supplied by the instrument manufacturer on a second laptop computer. It was found that some of the data collected from the pressure probes and load cells was contaminated with a 50Hz electrical interference from the overhead catenaries supplying power to the vehicles. Frequency analysis showed that the vehicle signal was entirely below this frequency and therefore all these data were double-filtered using a 40Hz 10-pole low-pass Butterworth filter before further processing.

Pressure and load cell data from 42 vehicle passes were successfully collected over a 2-day measuring period with 28 of those also being recorded with the Cobra Probe in one of the four positions. Some of these vehicle passes were also recorded by colleagues from the Southampton University using a combination of geophone and high-speed video recording to monitor track deflection and vibration in a manner similar to [12] although these data are not reported here. The data from each vehicle pass was extracted and the time base synchronised [5, 6] and non-dimensionalised by the speed of the vehicle such that the 20 car vehicle passes in a non-dimensional time of 20 units. (N.B. the two leading and two trailing cars of a Eurostar vehicle are longer than the intervening cars meaning this time parameter does not corre-

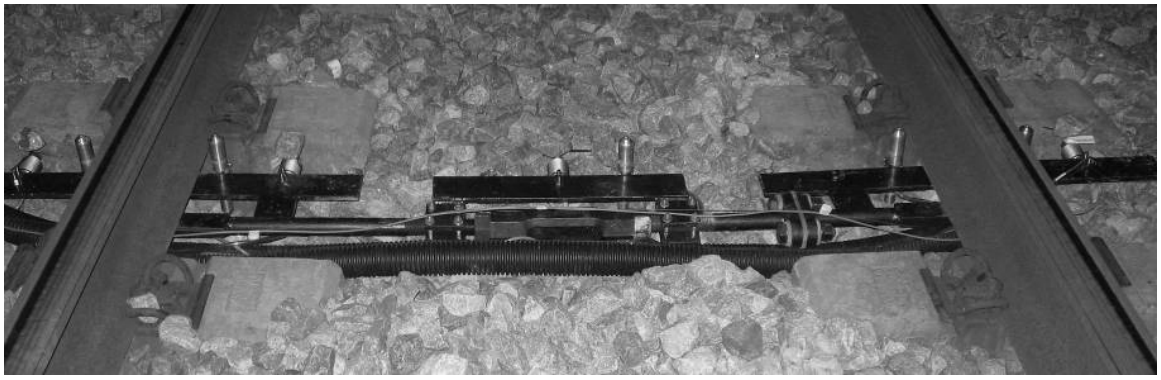

Figure 4 - Photograph of instrumented gauge bar installed on track. Visible are the upright static pressure probes in positions T1 to T5 (from right to left), the 4 horizontal load cells adjacent to T1, T3, T4 and T5. The Cobra probe is not shown in this photograph.

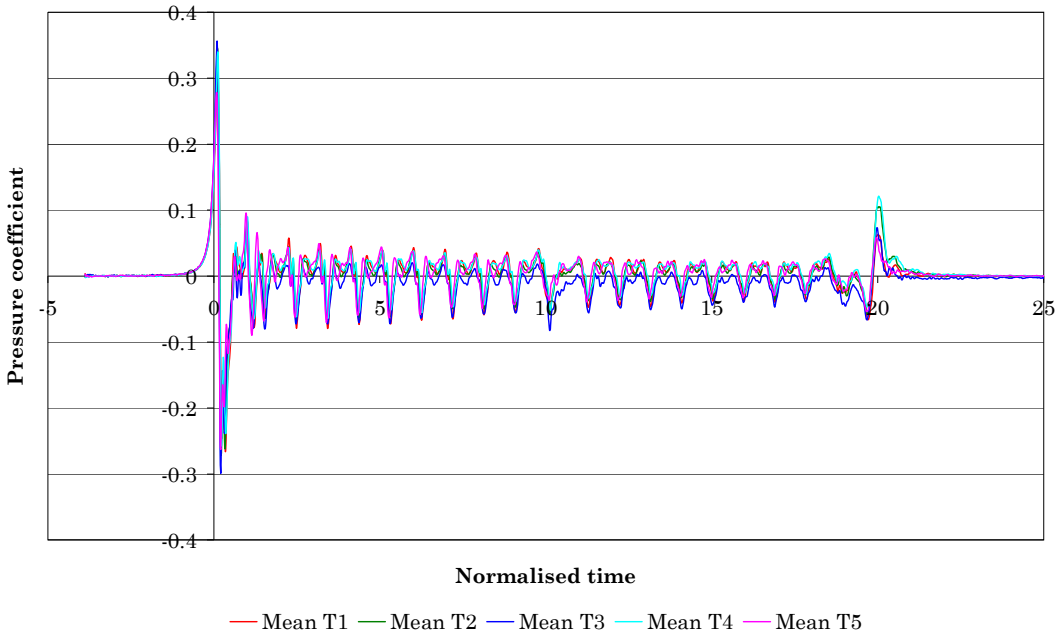

Figure 5 - Ensemble mean (n=42) static pressure for 5 positions across the track

spond precisely with actual car positions but can be taken as representative). The data were then also non-dimensionalised by the dynamic pressure or vehicle speed as appropriate and an ensemble formed from data in each instrument position.

3 RESULTS

Fig. (5) shows the ensemble pressure coefficient trace obtained from these measurements at the 5 positions across the track. The positions T1 to T5 correspond to the probes positioned from outside the rails nearest the centre of the trackbed (T1), inside the rail nearest the centre of the trackbed (T2), approximately central between the rails (T3), inside the rail nearest the shoulder of the trackbed (T4) and outside the rail on the shoulder of the trackbed (T5).

The basic form of the trace fits well with the results for other vehicle shapes / speeds [5]

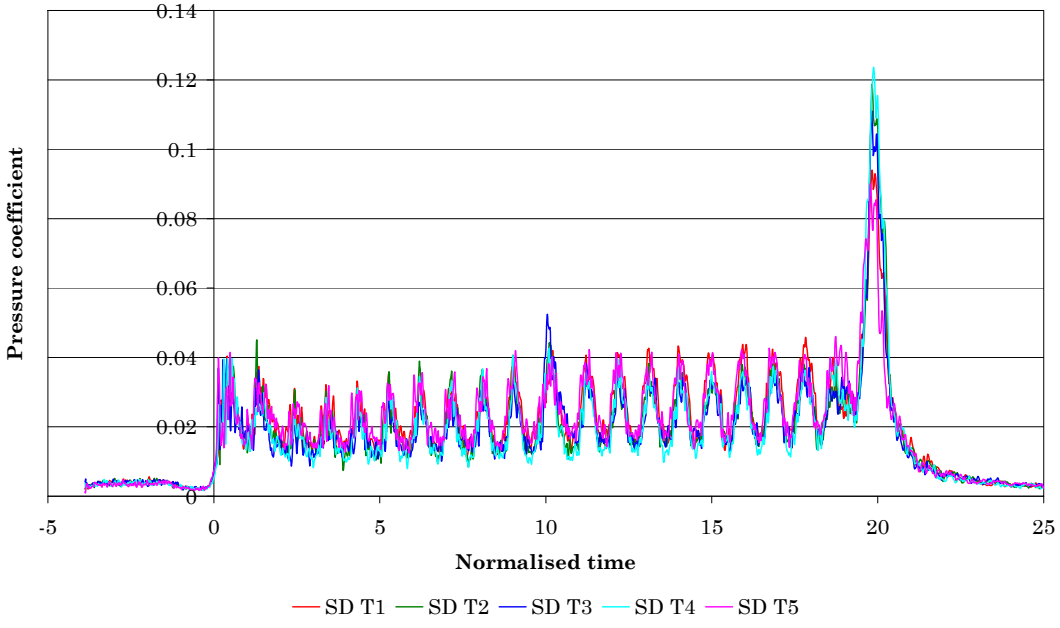

Figure 6 - Ensemble SD (n=42) static pressure for 5 positions across the track

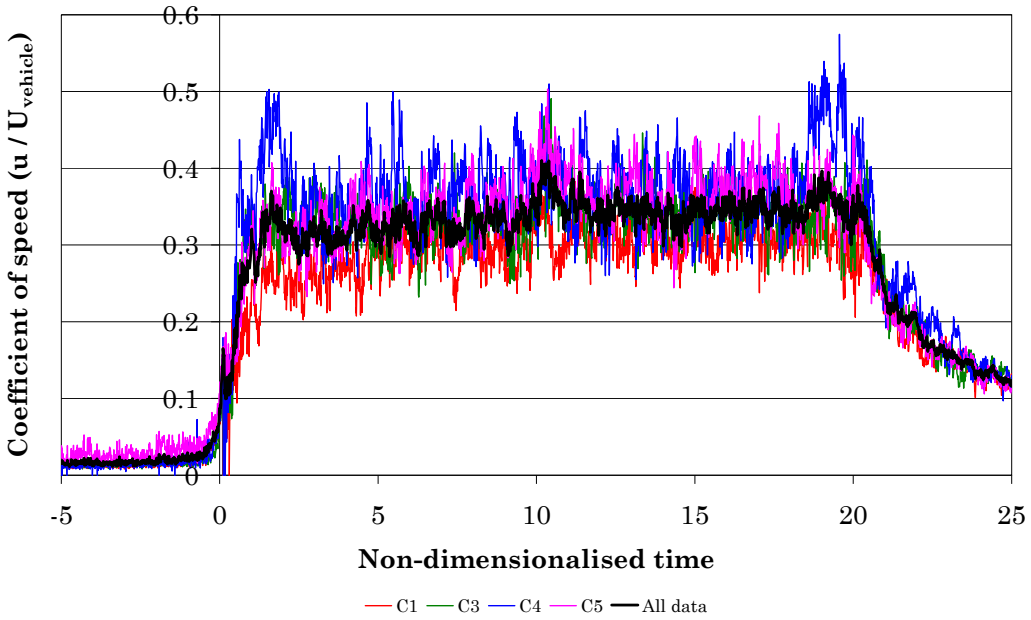

Figure 7 - Ensemble mean (n=8,7,5,8 total 28) along-vehicle air speed for 4 positions across the track

and is particularly interesting because of the clear peak of pressure at the vehicle-trailing end, which has not previously been reported at full-scale. This feature is repeatable and occurs in the ensemble average as well as the ensemble standard deviation (Fig. (6)), the latter only having been previously reported [5].

Both the ensemble mean and the SD show a high degree of correspondence with the geometry of the vehicle, particularly the unique articulated design of the passenger car bogies (with 1 bogie linking 2 cars rather than 2 separate bogies on each car) and the formation of the vehicle from two 10-car units joined in the centre [13]. This correspondence with vehicle geometry was also noticed by [7] in full-scale tests with a different vehicle and suggests that the detailed arrangement of bogies, inter-car spacing and other under-vehicle equipment may have a considerable impact on the levels of aerodynamic forces experienced by the trackbed. Additionally, there appears to be relatively small variation with track position compared to the within-vehicle variation.

The air speed measurements (Fig. (7)) include data from 4 positions approximately corresponding to the static pressure measurement locations T1, T3, T4 and T5. These also show relatively little variation with track position which may suggest the under body flow has less sensitivity to position than the free side / roof flow field [4, 5]. However, this lack of a consistent pattern contrasts with the profile of [9] and may be due to lack of data within the ensemble. The general form of the ensemble follows the five flow field regions identified in previous studies [6] and appears generally to scale with vehicle speed as expected. However, the coefficient of velocity was higher than expected with the streamwise component typically being in the range 0.3 to 0.4 (mean air speeds of around 25 ms^{-1} with peaks of over 40 ms^{-1}) approximately 50 mm above the ballast surface.

Direct comparison with other recently reported studies [7, 8] is difficult because of the differences in probe position and type. However, the general form, including the “spike” of reversed flow in the nose region and the positive “spike” at the tail, appears to be in agreement with both the full-scale measurements of [7, 8] and the model studies of [8]. The addi-

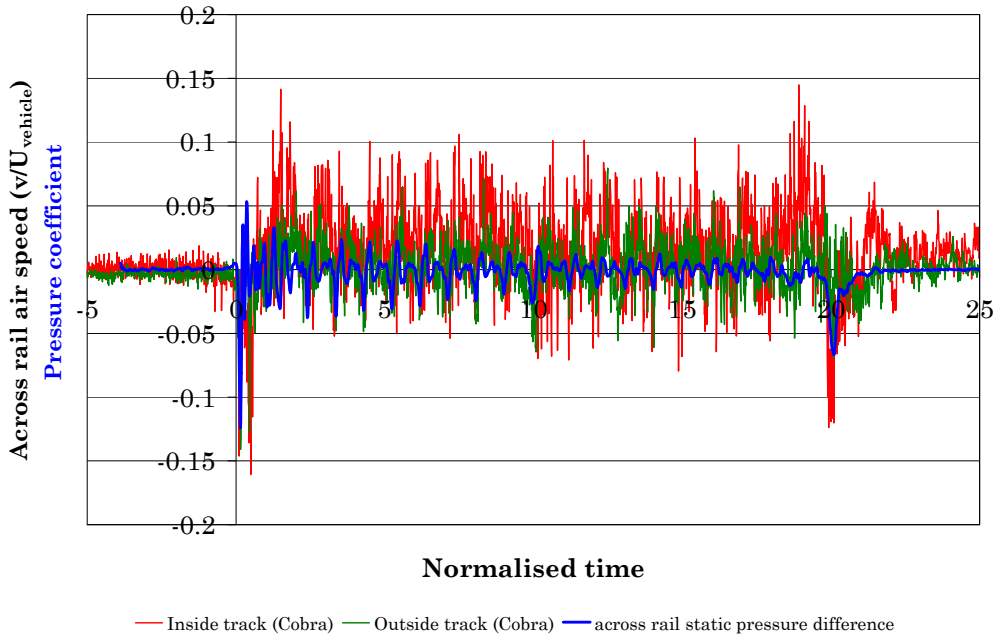

Figure 8 - Ensemble mean (n=5, 16) across track air flow measured with the Cobra probe inside and outside the rail with associated ensemble mean (n=42) static pressure difference

tional peak in the centre of the vehicle is again associated with the larger inter-car gap and different bogie arrangement where the two 10-car units are joined [13].

Measurements of the across-track component of airflow (Fig. (8)) suggest this is primarily associated with the nose and tail regions of the vehicle, where the flow is inward to the centre of the track, with lower flow magnitudes generally outward along the rest of the vehicle. In the nose region, the peak in across-track pressure differential (Fig. (8)) is associated with the nose region positive pressure pulse (Fig. (5)), which is also associated with the short duration drop in along-track flow (Fig. (7)) and is likely also associated with the flow reversal region reported by [7]. There appears to be momentary peak in across track airflow at this same time with a second peak occurring after this initial pulse.

In the tail region the differential pressure and across rail airflow peaks occur at the same time. This region also contains a peak in ensemble pressure (Fig. (5)) and intermittently in along-track air speed (Fig. (7)) with a large peak in the ensemble SD of static pressure (Fig. (6)). It has been suggested by [14] that these features may be linked to structured vortices in the near wake region but that the ensemble averaging techniques, as used here and in [14], are insufficient to enable a detailed analysis of this region because of the intermittency of such structures.

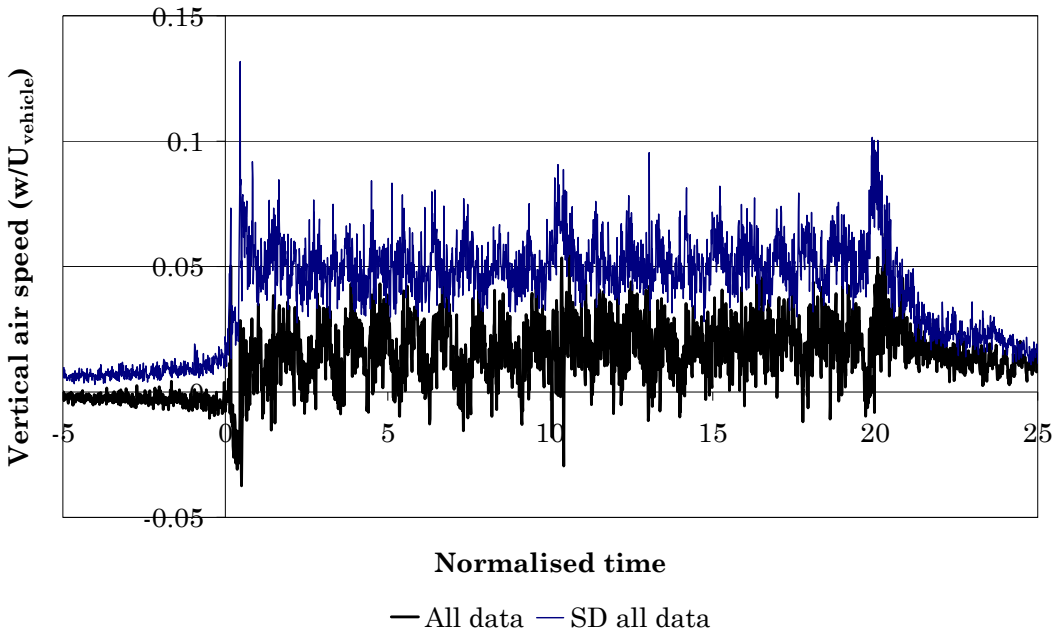

Figure 9 - Ensemble mean (n=28) and SD vertical air flow measured with the Cobra probe. Data from all 4 track positions has been combined in this figure.

The vertical component of air velocity also showed no consistent pattern with track position, although this again potentially due to lack of data within the ensemble. Fig. (9) therefore shows an ensemble of the vertical air speed at all 4 track positions. These data again demonstrate a correspondence with the 20-car geometry of the vehicle with particular peaks in the nose, tail and vehicle centre. The initial nose feature indicates a downward flow, which continues until the second peak in across track flow (Fig. (8)), after which the flow direction is generally upward. The peaks at the rear of the vehicle are again consistent with the idea of an intermittent trailing vortex structure [14].

4 DISCUSSION AND FURTHER WORK

The across-track airflows, when coupled with the significant along-vehicle airflows close to the ballast surface and associated pressure fluctuations, provides a potential mechanism for ballast particle transport onto the railhead where it could be crushed, causing ballast pitting. Such a mechanism would require at least two stages, an initial suspension of the particle and a subsequent movement onto the railhead. The load-cell measurements conducted as part of this study, and the vibration measurements of Southampton University, showed that there were significant vehicle related forces being generated on ballast particles but that these were not generally related to aerodynamic factors. Such forces are thought to be due to mechanical vibration of the trackbed by the vehicle [12] and potentially provide the suspension mechanism for particles, particularly in the nose region and when coupled to vertical airflow “gusts”. These particles may then be swept by aerodynamic forces onto the railhead where they are crushed by the vehicle.

Such a mechanism would imply that ballast-pitting events would be associated with the nose region of vehicles. Some supporting evidence for this, albeit circumstantial, comes from the inspection and maintenance of the vehicle wheels, which would be expected to be equally pitted from such ballast crushing events. Interviews by the authors with vehicle maintenance staff suggest that such wheel pitting occurs predominantly on the front and rear bogies with a

steady reduction toward the centre of the vehicle. This supports the idea of the mechanism being initiated by the approaching vehicle vibrations and continued by the under-body aerodynamic forces. The wheel pitting in the rear portion of the vehicle is then explained by the reversal of vehicle direction during the return journey.

Additional work is required to verify this theory. In particular, work should be focused on increasing the number of runs within each ensemble so that profiles of air velocity across the track and vertically, comparable with [9], can be produced. The existing data will also be used to model ballast particle behaviour to test the size of particles at greatest risk from this phenomenon. Such information might then be used to propose mitigation methods to reduce the maintenance costs associated with this phenomenon.

ACKNOWLEDGEMENTS

The authors would like to acknowledge the help and support of Network Rail (CTRL).

REFERENCES

[1] D. F. Cannon, K.-O. Edel, S. L. Grassie, K. Sawley. Rail defects: an overview. *Fatigue & Fracture of Engineering Materials and Structures*, **26**(10), 865–886, 2003.

[2] V. Reddy, G. Chattopadhyay, P-O Larsson-Kraik, D. J. Hargreaves. Modelling and analysis of rail maintenance cost. *International Journal of Production Economics*, **105**(2), 475-482, 2007.

[3] E. Magel, M. Roney, J. Kalousek, P. Sroba. The blending of theory and practice in modern rail grinding. *Fatigue & Fracture of Engineering Materials and Structures*, **26**(10), 921–929, 2003.

[4] P. M. Cali, E. F. Covert. Experimental measurements of the loads induced on an overhead highway sign structure by vehicle-induced gusts. *Journal of Wind Engineering and Industrial Aerodynamics*, **84**(1), 87-100, 2000.

[5] A. D. Quinn, C. J. Baker, N. G. Wright. Wind and vehicle induced forces on flat plates—Part 2: vehicle induced force. *Journal of Wind Engineering and Industrial Aerodynamics*, **89**(9), 831–847, 2001.

[6] C. J. Baker, S. J. Dalley, T. Johnson, A. Quinn, N. G. Wright. The slipstream and wake of a high speed train. Proceedings of the Institution of Mechanical Engineers Part F-Journal of Rail and Rapid Transit, **215**(2), 83-99, 2001.

[7] H.-J. Kaltenbach, P.-E. Gautier, G. Agirre, A. Orellano, K. Schroeder-Bodenstein, M. Testa and Th. Tielkes. Assessment of the aerodynamic loads on the trackbed causing ballast projection: results from the DEUFRAKO project Aerodynamics in Open Air (AOA). Proceedings of the World Congress on Rail Research, Seoul, South Korea, May 2008.

[8] A.Ido, S.Saitou, K.Nakade and S.Iikura. Study on under-floor flow to reduce ballast flying phenomena. Proceedings of the World Congress on Rail Research, Seoul, South Korea, May 2008.

[9] H. B. Kwon and C. S. Park. An experimental study on the relationship between ballast flying phenomenon and strong wind under high speed train. Proceedings of the World Congress on Rail Research, Montreal, Canada, 2006.

[10] C. J. Baker. Keynote lecture – The flow around high speed trains. Proceedings of the BBAA VI conference, Milano, Italy, 2008.

[11] P. Moran, R. P. Hoxey. A probe for sensing static pressure in two-dimensional flow. *Journal of Physics E: Scientific Instruments*, **12**(8), 752-753, 1979.

[12] D. Bowness, A.C. Lock, W. Powrie, J.A. Priest and D.J. Richards. Monitoring the dynamic displacements of railway track. *Proceedings of the IMechE Part F: J. Rail and Rapid Transport*, **221** F1, 13-22, 2007.

[13] Alstom. Eurostar: a TGV bridging nations. Available from http://www.transport.alstom.com/_eLibrary/brochure/upload_91523.pdf (last accessed 25/06/08)

[14] M. Sterling, C. J. Baker, S. C. Jordan and T. Johnson. A study of the slipstreams of high-speed passenger trains and freight trains. *Proceedings of the IMechE Part F: J. Rail and Rapid Transport*, **222** In Press 2008.